Journal of Materials Chemistry A

RSC Publishing

PAPER

View Article Online
View Journal | View Issue

Cite this: J. Mater. Chem. A, 2013, 1, 4858

A novel compact DPP dye with enhanced light harvesting and charge transfer properties for highly efficient DSCs†

Fang Zhang,[ab] Ke-Jian Jiang,*[a] Jin-Hua Huang,[a] Chun-Chun Yu,[a] Shao-Gang Li,[a] Ming-Gong Chen,*[b] Lian-Ming Yang[a] and Yan-Lin Song*[a]

Received 8th February 2013
Accepted 14th February 2013

DOI: 10.1039/c3ta10618g

www.rsc.org/MaterialsA

A novel compact diketopyrrolopyrrole (DPP) dye was designed and synthesized using DPP core as a bridge to connect bis(4-*tert*-butylphenyl)phenylamine and cyanoacetic acid units with the D–π–A configuration, and employed as a sensitizer in dye-sensitized solar cells, giving a high power conversion efficiency of 8.61% under AM 1.5 conditions.

Introduction

Dye-sensitized solar cells (DSCs) are one of the most promising alternatives to the conventional inorganic devices due to their potentially low material/fabrication cost and relatively high conversion efficiencies.[1] In DSCs, the sensitizer is one of the key components, exerting a significant influence on the device power conversion and stability. With ruthenium complexes[2a–d] and zinc porphyrin dyes,[2e,f] high power conversion efficiencies of up to 8–12% have been achieved. On the other hand, metal-free organic dyes, usually with the electron donor–π bridge–electron acceptor (D–π–A) configuration, have been actively pursued due to their molecular tailoring flexibility and raw material abundance.[3] In the D–π–A organic dyes, triarylamine and cyanoacrylic acid were widely used as a donor and an acceptor, respectively, and various π-conjugated bridges were employed to bridge the donor and acceptor units to create a large number of D–π–A dyes for DSCs. It is well known that the bridge is of paramount importance in tuning the molecular energy gap, and the electronic and steric structures, strongly affecting device performances.[4]

The diketopyrrolopyrrole (DPP) chromophore has a uniquely planar conjugated bicyclic structure with electron-withdrawing property, and its derivatives are extensively used as high-performance pigments due to its exceptional photochemical, mechanical and thermal stability.[5] Following its successful investigations in a series of optical electronic devices,[6] it was tested as a bridge to construct D–π–A organic dyes for DSCs recently,[7] and the device performances have been greatly improved since the report in 2010.[7a] Recently, Han's group introduced a strong electron donor indoline into a DPP dye, giving an efficiency of 7.4%.[7d] Very recently, an asymmetric DPP sensitizer with intense absorption in the red/near-IR region was prepared with an efficiency of 7.7%, and a higher efficiency of 8.6% was achieved by its co-sensitization with another organic sensitizer with complementary spectral absorption in the visible region.[7f] Thus, DPP is a desirable building block for constructing highly efficient sensitizers in DSCs.

In this article, we demonstrate a successful design of a new metal-free organic dye, utilizing the DPP core as the π-conjugated bridge, bis(4-*tert*-butylphenyl)phenylamine as the electron donor and cyanoacrylic acid as the electron acceptor/anchoring group (denoted as **ICD-1**). For comparison, a reference sensitizer was synthesized with an additional phenyl unit inserted between the triphenylamine unit and DPP core (denoted as **ICD-2**), whose structure was extensively studied in DPP-based sensitizers recently.[7] Our experiment showed that, without the phenyl unit, the dye absorption band in **ICD-1** is dramatically red-shifted with highly enhanced molar coefficient efficiency, and the power conversion efficiency was significantly improved from 7.20% (**ICD-2**) to 8.61% (**ICD-1**) in DSCs with an I^-/I_3^- based electrolyte under standard AM 1.5 conditions.

Experimental section

Measurement and characterization

NMR spectra were recorded on a BRUKER AVANCE 400 MHz instrument. The residual solvent protons (^1H) or the solvent carbons (^{13}C) were used as internal standards. ^1H-NMR data are presented as follows: the chemical shift in ppm (δ) downfield from tetramethylsilane (multiplicity, coupling constant (Hz), integration). The following abbreviations are used in reporting NMR data: s, singlet; br.s, broad singlet; d, doublet; t, triplet; q, quartet; dd, doublet of doublets; and m, multiplet. UV-vis absorption spectra were recorded on a HP 8453

[a]Laboratory of New Materials, Institute of Chemistry, Chinese Academy of Sciences, Beijing, P. R. China, 100190. E-mail: kjjiang@iccas.ac.cn; ylsong@iccas.ac.cn
[b]School of Chemical Engineering of Anhui University of Science and Technology, Huainan, P. R. China, 232001. E-mail: mgchen@aust.edu.cn

† Electronic supplementary information (ESI) available. See DOI: 10.1039/c3ta10618g

spectrophotometer. Mass spectra were taken on a Bruker Daltonics Inc. APEXII FT-ICR spectrometer. The photocurrent–voltage (*I–V*) characteristics were recorded at room temperature using a computer-controlled Keithley 2400 source meter under air mass (AM) 1.5 simulated illumination (100 mW cm^{-2}, Oriel, 67005). The action spectra of the monochromatic incident photo-to-current conversion efficiency (IPCE) for solar cells were collected using a commercial setup (PV-25 DYE, JASCO). A 300 W Xenon lamp was employed as light source for generation of a monochromatic beam. Calibrations were performed with a standard silicon photodiode. IPCE is defined as $IPCE(\lambda) = hcJ_{sc}/e\varphi\lambda$, where h is Planck's constant, c is the speed of light in a vacuum, e is the electronic charge, λ is the wavelength in meters (m), J_{sc} is the short-circuit photocurrent density (A m^{-2}), and φ is the incident radiation flux (W m^{-2}).

Materials

All reagents were obtained from Alfa Aesar Chemical Co., Aladdin Chemical Co., and J&K Chemical Co. and they were used as received unless otherwise specified. All manipulations involving air-sensitive reagents were performed in an atmosphere of dry argon. The solvents (tetrahydrofuran (THF) and toluene) were purified by routine procedures and were distilled under dry argon before being used. 1,4-Diketo-3,6-bis(4-bromophenyl)pyrrolo[3,4-*c*]-pyrrole (DPP) was prepared according to the reference procedures.[8]

Synthesis of 2. An oven-dried 250 mL one-necked flask was charged with DPP (**1**) (3.6 g, 8 mmol), NaH (0.48 g, 20 mmol) (60% dispersion in mineral oil, in soluble bags in resealable cans) and 150 mL of DMF. The mixture was stirred for 1 h at room temperature, followed by dropping 1-bromohexane (13.3 g, 80 mmol) in 30 mL of DMF. The mixture was kept for an additional 30 h at room temperature and filtered. The solid was washed with 60 mL of chloroform, and the organic phase was washed with water (3 × 50 mL) and brine (3 × 50 mL). The combined organic phase was evaporated under reduced pressure and the residue was purified by silica-gel column chromatography to give an orange-red polycrystalline powder (2.2 g, yield = 45%). ^{1}H-NMR ($CDCl_3$; 400 MHz), δ (ppm): 0.83 (t, J = 6.8 Hz, 6H), 1.20–1.30 (m, 12H), 1.52–1.58 (m, 4H), 3.72 (t, J = 7.6 Hz, 4H), 7.67 (s, 8H).

Synthesis of 3. An oven-dried 100 mL three-necked flask was charged with compound **2** (1.84 g, 3 mmol), $Pd(PPh_3)_4$ (0.24 g, 0.21 mmol), and sodium carbonate (5.4 g, 51 mmol). The flask was evacuated and backfilled with nitrogen, with the operation being repeated twice. 40 mL of THF and 15 mL of H_2O were added and the blend was heated at 45 °C for 0.5 h, then a solution of 5-formyl-2-thiophenylboronic acid (0.47 g, 3.0 mmol) in 10 mL of THF was added using a syringe at this time. The temperature was increased to 80 °C and maintained for 16 h. After cooling to room temperature, dichloromethane was added and the organic phase was filtered through a silica-gel pad. The filtrate was washed with water (3 × 20 mL) and brine (3 × 20 mL). The combined organic phase was dried on $MgSO_4$, filtered and evaporated under reduced pressure and the residue was purified by silica-gel column chromatography to give an orange-red fraction corresponding to pure compound **3** (0.81 g, yield = 42%). ^{1}H-NMR ($CDCl_3$; 400 MHz), δ (ppm): 0.83 (m, 6H), 1.22 (s, 12H), 1.55–1.60 (m, 4H), 3.71–3.80 (m, 4H), 7.50 (d, J = 4 Hz, 1H), 7.65–7.71 (m, 4H), 7.77 (d, J = 4 Hz, 1H), 7.80 (d, J = 8.4 Hz, 2H), 7.89 (d, J = 8.4 Hz, 2H), 9.92 (s, 1H).

Synthesis of 4. An oven-dried 100 mL three-necked flask was charged with compound **3** (0.64 g, 1.0 mmol), $Pd(OAc)_2$ (22 mg, 0.1 mmol), P(*t*-Bu)$_3$ (20 mg, 0.1 mmol), bis(4-(*tert*-butyl)phenyl) amine (0.37 g, 1.30 mmol) and ^{t}BuONa (0.48 g, 5.0 mmol). The flask was evacuated and backfilled with nitrogen, with the operation being repeated twice. Then 20 mL of toluene were added and the mixture was heated at 90 °C for 16 h. After cooling to room temperature, dichloromethane was added and the organic phase was filtered through a silica-gel pad. The filtrate was washed with water (3 × 20 mL) and brine (3 × 20 mL). The combined organic phase was dried on $MgSO_4$, filtered and evaporated under reduced pressure and the residue was purified by silica-gel column chromatography to give a purple solid (0.53 g, 62%). ^{1}H-NMR ($CDCl_3$, 400 MHz) δ (ppm): 0.81–0.88 (m, 6H), 1.23–1.28 (m, 12H), 1.33 (s, 18H), 1.61–1.74 (m, 4H), 3.79 (t, J = 7.8 Hz, 4H), 7.03 (d, J = 8.8 Hz, 2H), 7.13 (d, J = 8.8 Hz, 4H), 7.34 (d, J = 8.8 Hz, 4H), 7.49 (d, J = 4 Hz, 1H), 7.77–7.82 (m, 5H), 7.90 (d, J = 8.8 Hz, 2H), 9.92 (s, 1H).

Synthesis of ICD-1. An oven-dried 100 mL one-necked flask was charged with compound **4** (3.5 × 10^{-4} mol), cyanoacrylic acid (7 × 10^{-3} mol), 10 mL of dry THF and 0.4 mL piperidine. The solution was heated to reflux for 15 h and the colour turned deep red. After cooling to room temperature, dichloromethane was added and the organic phase was washed with water (3 × 20 mL) and brine (3 × 20 mL). The combined organic phase was dried on $MgSO_4$, filtered and evaporated under reduced pressure and the residue was purified by silica-gel column chromatography to give a purple solid (86%). ^{1}H-NMR (DMSO, 400 MHz) δ (ppm): 0.75–0.85 (m, 6H), 1.12–1.16 (m, 12H), 1.29 (s, 18H), 1.47 (s, 4H), 3.71 (s, 4H), 6.84 (d, J = 8 Hz, 2H), 7.10 (d, J = 8.4 Hz, 4H), 7.41 (d, J = 8.4 Hz, 4H), 7.77–7.80 (m, 4H), 7.88 (s, 4H), 8.18 (s, 1H); HRMS (ESI): *m*/*z* found (M + 1): 913.4696.

Synthesis of 5. An oven-dried 100 mL three-necked flask was charged with compound **3** (0.64 g, 1 mmol), $Pd(PPh_3)_4$ (81 mg, 0.07 mmol), and Na_2CO_3 (2.3 g, 0.02 mol). The flask was evacuated and backfilled with nitrogen, with the operation being repeated twice. 30 mL of THF and 8 mL of H_2O were added and the blend was heated at 45 °C for 0.5 h, then a solution of bis(4-(*tert*-butylphenyl)amino)phenyl boronic acid (0.61 g, 1.50 mmol) in 10 mL of THF was added using a syringe at this time. The temperature was increased to 80 °C and maintained for 16 h. After cooling to room temperature, dichloromethane was added and the organic phase was filtered through a silica-gel pad. The filtrate was washed with water (3 × 20 mL) and brine (3 × 20 mL). The combined organic phase was dried on $MgSO_4$, filtered and evaporated under reduced pressure and the residue was purified by silica-gel column chromatography to give a red solid (0.31 g). Yield: 36%. ^{1}H-NMR ($CDCl_3$, 400 MHz) δ (ppm): 0.83 (t, J = 6.4 Hz, 6H), 1.24 (s, 12H), 1.33 (s, 18H), 1.64–1.65 (m, 4H), 3.78–3.84 (m, 4H), 7.08 (d, J = 8.8 Hz, 4H), 7.12 (d, J = 8.8 Hz, 2H), 7.31 (d, J = 8.8 Hz, 4H), 7.50–7.52 (m, 3H), 7.72 (d, J = 8.4 Hz, 2H), 7.78 (d, J = 3.6 Hz, 1H), 7.83 (d, J = 8.8 Hz, 2H), 7.92 (t, J = 7.8 Hz, 4H), 9.28 (s, 1H).

Synthesis of ICD-2. An oven-dried 100 mL one-necked flask was charged with compound **5** (3.5×10^{-4} mol), cyanoacrylic acid (7×10^{-3} mol), 10 mL of dry THF and 0.4 mL piperidine. The solution was heated to reflux for 15 h and the colour turned deep red. After cooling to room temperature, dichloromethane was added and the organic phase was washed with water (3×20 mL) and brine (3×20 mL). The combined organic phase was dried on $MgSO_4$, filtered and evaporated under reduced pressure and the residue was purified by silica-gel column chromatography to give a purple solid (86%). ^{1}H-NMR ($CDCl_3$, 400 MHz) δ (ppm): 0.82 (t, $J = 7.2$ Hz, 6H), 1.20–1.25 (m, 12H), 1.33 (s, 18H), 1.58 (s, 4H), 3.72–3.83 (m, 4H), 7.07–7.11 (m, 6H), 7.29 (d, $J = 8.8$ Hz, 4H), 7.47–7.50 (m, 3H), 7.68–7.70 (m, 3H), 7.76–7.80 (m, 4H), 7.86 (d, $J = 8.4$ Hz, 2H), 8.05 (s, 1H); HRMS (ESI): m/z found (M + 1): 989.5036.

DSC fabrication

The nanocrystalline TiO_2 pastes (particle size, 20 nm) were prepared using a previously reported procedure.[9] Fluorine doped thin oxide (FTO, 4 mm thickness, 10 ohm sq^{-1}, Nippon Sheet Glass, Japan) conducting electrodes were washed with soap and water, followed by sonication for 10 min in acetone and isopropanol, respectively. Following a drying period, the electrodes were submerged in a 40 mM aqueous solution of $TiCl_4$ for 30 min at 75 °C, and then washed by water and ethanol. On the electrodes, an 11 μm thick nanocrystalline TiO_2 layer and a 6 μm thick TiO_2 light scattering layer (particle size, 400 nm, PST-400C) were prepared by the screen-printing method. The TiO_2 electrodes were heated at 500 °C for 30 min, followed by treating with a 40 mM aqueous solution of $TiCl_4$ for 30 min at 75 °C and subsequent sintering at 500 °C for 30 min. The thickness of TiO_2 films was measured using a profiler, Sloan, Dektak3.

The electrodes were immersed in a dye bath containing 0.2 mM **ICD-1** or **ICD-2** and 20 mM 3α,7α-dihydroxy-5β-cholic acid (chenodeoxycholic acid) in 4-*tert*-butanol–acetonitrile mixture–tetrahydrofuran (1 : 1 : 0.2, v/v) and kept for 24 h at room temperature. The dyed electrodes were then rinsed with the mixed solvent to remove the excess dye. A platinum-coated counter electrode was prepared according to a previous report,[10] and two holes were drilled on its opposite sides. The two electrodes were sealed together with a 25 μm thick thermoplastic Surlyn frame. An electrolyte solution was then introduced through one of the two holes in the counter electrode, and the holes were sealed with the thermoplastic Surlyn. The electrolyte contains 0.68 M dimethyl imidazolium iodide, 0.05 M iodine, 0.10 M LiI, 0.05 M guanidinium thiocyanate, and 0.40 M *tert*-butylpyridine in the mixture of acetonitrile and valeronitrile (85 : 15, v/v). All the devices were prepared with a photoactive area of about 0.3 cm^2, and a metal mask of 0.165 cm^2 was used to cover the device for photovoltaic property measurements.

Results and discussion

Optical and electrochemical properties

The synthetic routes to **ICD-1** and **ICD-2** are described in Scheme 1. Their UV-Vis absorption spectra examined in dichloromethane solutions and on a transparent TiO_2 film (4.5 μm) are displayed in Fig. 1, and the relevant parameters are collected in Table 1. Both the dyes showed broad absorption spectra with two absorption bands covering a wide range in the visible region. Interestingly, the longer wavelength band of **ICD-1** ($\lambda_{max} = 543$ nm), assigned to intramolecular charge transfer (ICT), is significantly red-shifted compared to that of **ICD-2** ($\lambda_{max} = 519$ nm), although **ICD-2** has one additional phenyl ring. The UV-Vis spectra of dyes **ICD-1** and **ICD-2** adsorbed on transparent TiO_2 films were recorded and are shown in Fig. 2, where the CT bands of **ICD-1** and **ICD-2** were slightly blue-shifted with λ_{max} at 528 nm and 514 nm, respectively, compared to the solution spectra. Moreover, the molar extinction coefficient of **ICD-1** ($\varepsilon = 48\,100$ L mol^{-1} cm^{-1}) is higher than that of **ICD-2** ($\varepsilon = 43\,200$ L mol^{-1} cm^{-1}). The results imply that the

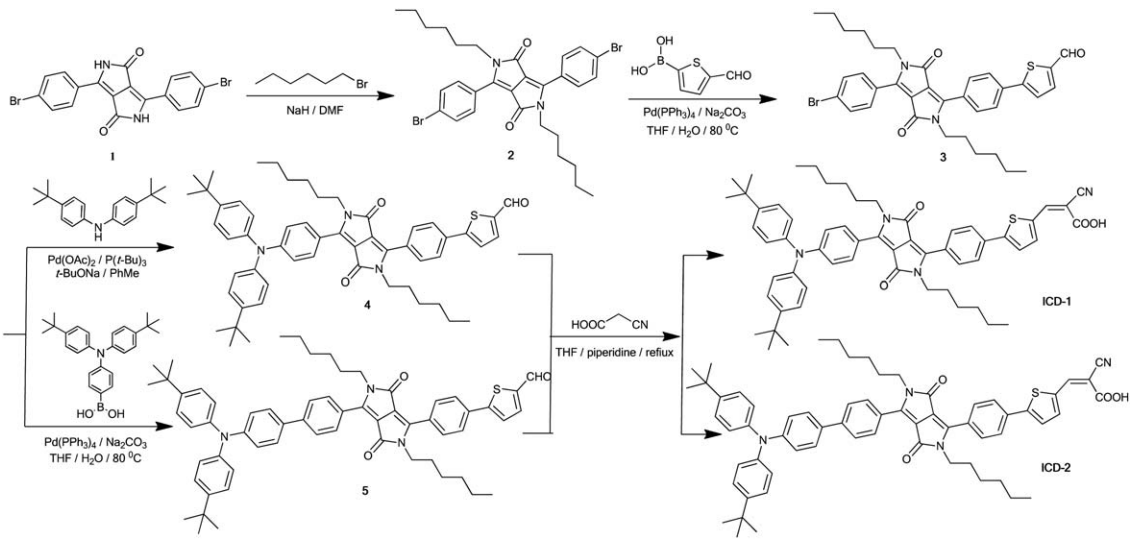

Scheme 1 The synthetic routes to **ICD-1** and **ICD-2**.

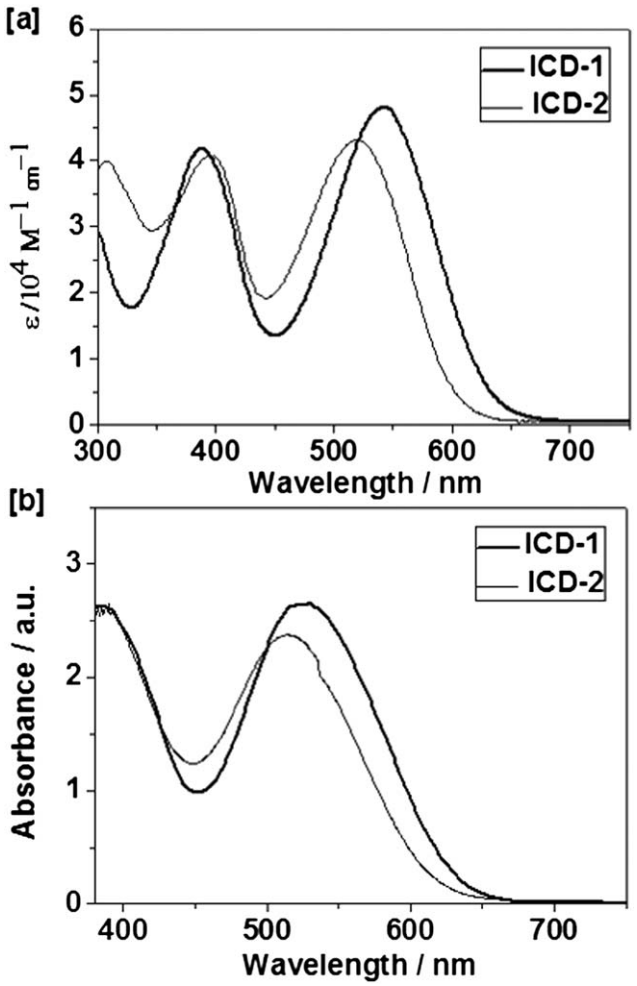

Fig. 1 Absorption spectra of **ICD-1** and **ICD-2** in dichloromethane (a) and on a transparent TiO_2 film (4.5 μm) (b).

device with **ICD-1** would harvest more photons and give a higher conversion efficiency as compared to the **ICD-2** based device. In general, the ICT band is strongly related to the nature of electron donor, acceptor, and the bridge connecting them in a D–π–A system. Thus, the ICT in **ICD-1** is more efficient than that in **ICD-2**. In this case, the additional benzene ring between the donor and DPP units is not an effective conjugation bridge for electron transfer in **ICD-2**. The reason could be explained by the presence of a non-planar biphenyl structure, which would hinder charge transfer from the donor to acceptor in the molecule.[11]

To investigate the molecular energy levels, cyclic voltammetry measurements were performed in a 0.1 M dichloromethane solution of tetra-*n*-butylammonium hexafluorophosphate with ferrocene as an internal standard at 0.63 V *vs.* NHE. The first oxidation potentials ($E_{+/0}$) of **ICD-1** and **ICD-2** were observed to be 0.97 and 0.99 V *vs.* NHE, respectively, which are assigned to the oxidation of triphenylamine units. The positive shift of the oxidation potential in **ICD-2** means the weaker donor–acceptor interaction due to poor charge transfer from triphenylamine to cyanoacetic acid, in keeping with the analysis presented above. Both the potential values are substantially more positive than that of the iodide/triiodide couple redox (0.4 V *vs.* NHE), indicating that the ground-state sensitizer regeneration is energetically favorable in DSCs.[12] The optical transition energies (E_{0-0}) were 2.04 eV for **ICD-1** and 2.12 eV for **ICD-2**, estimated from the intersection of their absorption and emission spectra. The excited-state redox potentials, $E_{+/*}$, determined by subtracting E_{0-0} from $E_{+/0}$, were −1.07 V for **ICD-1** and −1.13 eV for **ICD-2**. Both the values are negative enough to allow their excited state electron transfer into the TiO_2 conduction band (−0.5 V *vs.* NHE).[13]

Fig. 2 shows the action spectra in the form of monochromatic incident photon-to-current conversion efficiencies (IPCEs). The **ICD-1** based device clearly exhibited a stronger and broader response in the entire visible spectral region, especially in the red region, as compared to that of the **ICD-2** based device. The former showed plateaus of over 80% from 450 to 630 nm with the highest value of 87% at 600 nm and an onset at 800 nm, while **ICD-2** presented a relatively narrow response spectrum with the highest value of 82% at 543 nm. The difference between IPCE spectra is in good agreement with their difference in absorption spectra as shown in Fig. 1. The higher IPCE values for **ICD-1** in the whole spectrum imply efficient charge transfer upon photo-excitation, partly due to the efficient electron communication, as discussed above.

Table 1 Photoelectrochemical properties of **ICD-1** and **ICD-2** and their solar cell performances

Dye	λ_{max}[a] (nm)	ε (L mol^{-1} cm^{-1})	λ_{em}[b] (nm)	E_{0-0}[c] (eV)	$E_{+/0}$[d] (V)	$E_{+/*}$[e] (V)	J_{sc} (mA cm^{-2})	V_{oc} (mV)	FF	η[f] (%)
ICD-1	543	48 100	652	2.04	0.97	−1.07	16.65 ± 0.20	708 ± 10	0.73 ± 0.02	8.61
	389	41 900								
ICD-2	519	43 200	664	2.12	0.99	−1.13	13.67 ± 0.20	712 ± 10	0.74 ± 0.02	7.20
	393	41 000								

[a] Absorption in CH_2Cl_2 solutions (1×10^{-5} M) at rt. [b] Emission in CH_2Cl_2 solutions (1×10^{-5} M) at rt. [c] E_{0-0} values were estimated from the intersection of the absorption and emission spectra. [d] The oxidation potentials of the dyes were measured in CH_2Cl_2 solutions with tetra-butylammoniumhexafluorophosphate ($TBAPF_6$, 0.1 M) as an electrolyte, Pt wires as working and counter electrodes, Ag/Ag^+ as a reference electrode; calibrated with ferrocene/ferrocenium (Fc/Fc^+) as an internal reference and converted to NHE by addition of 630 mV. [e] The estimation was determined by subtracting E_{0-0} from $E_{s+/0}$. [f] The data were recorded under AM 1.5 G simulated solar light at a light intensity of 100 mW cm^{-2}, and represent the average of three devices, where TiO_2 films with a 11 μm thick nanocrystalline layer and a 6 μm thick scattering layer were used with an electrolyte containing 0.68 M dimethyl imidazolium iodide, 0.05 M iodine, 0.10 M LiI, 0.05 M guanidinium thiocyanate, and 0.40 M *tert*-butylpyridine in a mixture of acetonitrile and valeronitrile (85/15, v/v), and each value was averaged by three parallel samples.

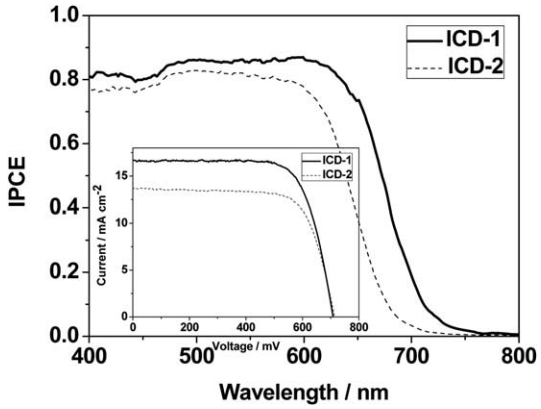

Fig. 2 IPCE spectra of DSCs with **ICD-1** and **ICD-2**, the inset shows their current–voltage characteristics.

The inset in Fig. 2 shows the energy conversion efficiency for DSCs with **ICD-1** and **ICD-2** under AM 1.5 G simulated solar light at a light intensity of 100 mW cm^{-2}. The **ICD-1** based-device gave a short circuit photocurrent density (J_{sc}) of 16.65 ± 0.20 mA cm^{-2}, an open circuit voltage (V_{oc}) of 708 ± 10 mV, and a fill factor (FF) of 0.73 ± 0.02, corresponding to an overall conversion efficiency (η), derived from the equation $\eta = J_{sc}V_{oc}FF$/light intensity, of 8.61%, while the **ICD-2** based device gave a J_{sc} of 13.67 ± 0.20 mA cm^{-2}, V_{oc} of 712 ± 10 mV, FF of 0.74 ± 0.02, and η of 7.20% under the same conditions. The large difference in the efficiency comes mainly from the differences in the J_{sc} between them. The higher J_{sc} for **ICD-1** is consistent with its higher and broader IPCE spectrum as compared with that for **ICD-2**. The comparison between **ICD-1** and **ICD-2** clearly reflects the importance of molecular configuration in the performance.

Density functional theory calculations

In order to gain insight into the geometrical configuration and electron distribution of the frontier orbitals of the two dyes, density functional theory (DFT) calculations were made on a B3LYP/6-31G level. Their optimized ground state molecular structures and the corresponding dihedral angles are presented in Fig. 3. As expected, the additional phenyl unit in **ICD-2** caused an additional torsion in the biphenyl unit with a dihedral angle of ≈32°. Correspondingly, the electron distribution of the HOMO is obstructed by the additional phenyl unit, and located mainly on the separate triphenylamine and DPP units in **ICA-2** as shown in Fig. 4. By contrast, the HOMO of **ICD-1** is homogeneously delocalized over the whole triphenylamine and DPP units. For both dyes, the LUMO orbitals show a similar electron distribution over the DPP core, phenyl unit, thiophene unit, and cyanoacetic acid unit with little contribution from the former. According to the observation, electron communication may be more favorable between the donor and acceptor in **ICD-1**, allowing an efficient electron transfer from the dye to TiO_2 electrode under light irradiation, which may result in a higher device performance as compared with that for **ICD-2**.

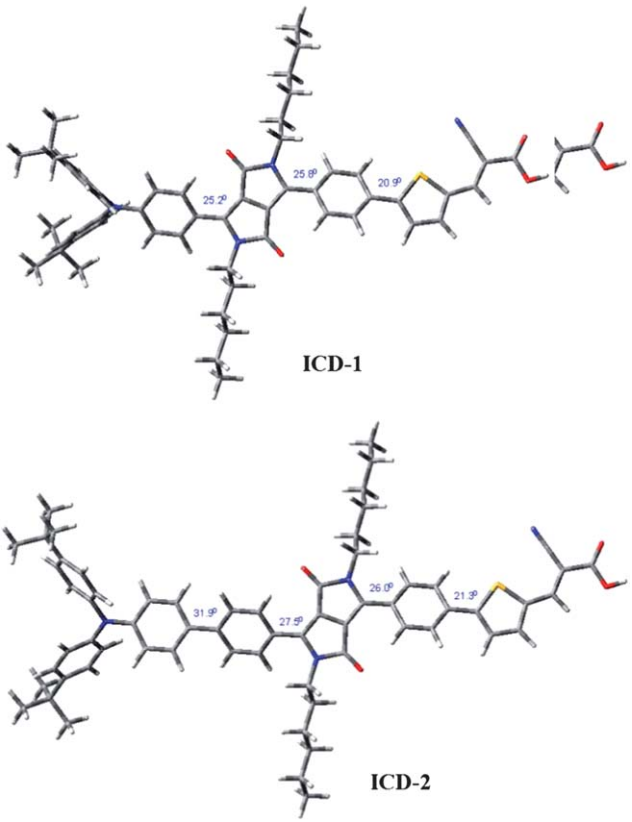

Fig. 3 The geometry optimized ground state molecular structures of **ICD-1** and **ICD-2** with the corresponding dihedral angles between each plain.

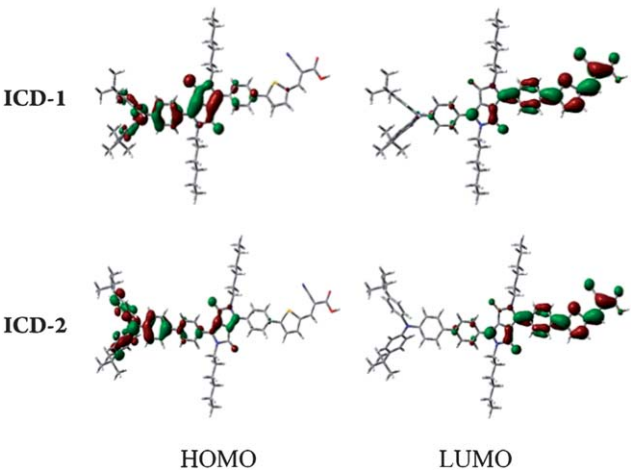

Fig. 4 HOMO–LUMO frontier molecular orbitals of **ICD-1** and **ICD-2**, calculated with DFT on a B3LYP/6-31+G(d) level (isodensity = 0.03 au).

Conclusions

In summary, a novel compact DPP-based dye **ICD-1** was designed and employed as a sensitizer in DSCs, giving a high power conversion efficiency of 8.61%, which is much higher than that (7.20%) for the reference dye with an additional phenyl unit inserted between the triphenylamine unit and DPP core, whose structure was extensively studied in DPP-based

sensitizers recently. Our results indicate that molecular engineering is crucial for constructing highly efficient sensitizers in DSCs, and the results would provide valuable, basic guidelines for rational designs of D–π–A molecules for high-performance DSCs and other optoelectronic devices. Further improvement of the performance could be expected for DPP sensitizers with a broader spectral response in the red/near-infrared region, and the research is in progress along with the stability test.

Acknowledgements

The authors greatly appreciate the financial support from the National Natural Science Foundation of China (Grant no. 21174149, 51173190, 21073203, 21076002 and 21121001), the National 863 Program (no. 2011AA050521), the 973 Program (2009CB930404, 2011CB932303, 2011CB808400), and the Scientific Equipment Program, ACS (YZ201106).

References

1 B. O'Regan and M. Grätzel, *Nature*, 1991, **353**, 737.
2 (*a*) M. K. Nazeeruddin, F. D. Angelis, S. Fantacci, A. Selloni, G. Viscardi, P. Liska, S. Ito, B. Takeru and M. Grätzel, *J. Am. Chem. Soc.*, 2005, **127**, 16835; (*b*) Y. Chiba, A. Islam, Y. Watanabe, R. Komiya, N. Koide and L. Han, *J. Appl. Phys.*, 2006, **45**, L638; (*c*) F. Gao, Y. Wang, D. Shi, J. Zhang, M. Wang, X. Jing, R. Humphry-Baker, P. Wang, S. M. Zakeeruddin and M. Grätzel, *J. Am. Chem. Soc.*, 2008, **130**, 10720; (*d*) K.-J. Jiang, N. Masaki, J. Xia, S. Noda and S. Yanagida, *Chem. Commun.*, 2006, 2460; (*e*) A. Yella, H. W. Lee, H. N. Tsao, C. Y. Yi, A. K. Chandiran, M. K. Nazeeruddin, E. W. G. Diau, C. Y. Yeh, S. M. Zakeeruddin and M. Grätzel, *Science*, 2011, **334**, 629; (*f*) Y.-C. Chang, C.-L. Wang, T.-Y. Pan, S.-H. Hong, C.-M. Lan, H.-H. Kuo, C.-F. Lo, H.-Y. Hsu, C.-Y. Lin and E. W.-G. Diau, *Chem. Commun.*, 2011, **47**, 8910.
3 (*a*) K. Hara, K. Sayama, Ya. Ohga, A. Shinpo, S. Suga and H. Arakawa, *Chem. Commun.*, 2001, 569; (*b*) S. Kim, J. K. Lee, S. O. Kang, J. Ko, J. H. Yum, A. Fantacci, F. D. Angelis, D. D. Censo, M. K. Nazeeruddin and M. Grätzel, *J. Am. Chem. Soc.*, 2006, **128**, 16701; (*c*) Y. Bai, J. Zhang, D. Zhou, Y. Wang, M. Zhang and P. Wang, *J. Am. Chem. Soc.*, 2011, **133**, 11442; (*d*) S. Li, K.-J. Jiang, K. Shao and L. Yang, *Chem. Commun.*, 2006, 2792; (*e*) T. Horiuchi, H. Miura, K. Sumioka and S. Uchida, *J. Am. Chem. Soc.*, 2004, **126**, 12218; (*f*) D. P. Hagberg, T. Edvinsson, T. Marinado, G. Boschloo, A. Hagfeldt and L. Sun, *Chem. Commun.*, 2006, 2245; (*g*) S. Ito, H. Miura, S. Uchida, M. Takata, K. Sumioka, P. Liska, P. Comte, P. Pechy and M. Gratzel, *Chem. Commun.*, 2008, 5194; (*h*) T. Bessho, S. M. Zakeeruddin, C.-Y. Yeh, E. W.-G. Diau and M. Graetzel, *Angew. Chem., Int. Ed.*, 2010, **49**, 6646; (*i*) W. Zeng, Y. Cao, Y. Bai, Y. Wang, Y. Shi, M. Zhang, F. Wang, C. Pan and P. Wang, *Chem. Mater.*, 2010, **22**, 1915; (*j*) N. Koumura, Z.-S. Wang, S. Mori, M. Miyashita, E. Suzuki and K. Hara, *J. Am. Chem. Soc.*, 2006, **128**, 14256.
4 (*a*) S. Haid, M. Marszalek, A. Mishra, M. Wielopolski, J. Teuscher, J.-E. Moser, R. Humphry-Baker, S. M. Zakeeruddin, M. Grätzel and P. Bäuerle, *Adv. Funct. Mater.*, 2012, **22**, 1291; (*b*) N. Cai, R. Z. Li, Y. L. Wang, M. Zhang and P. Wang, *Energy Environ. Sci.*, 2013, **6**, 139–147.
5 S. Qu and H. Tian, *Chem. Commun.*, 2012, **48**, 3039.
6 (*a*) M. Fukuda, K. Kodama, H. Yamamoto and K. Mito, *Dyes Pigm.*, 2004, **63**, 115; (*b*) Z. Qiao, Y. Xu, S. Lin, J. Peng and D. Cao, *Synth. Met.*, 2010, **160**, 1544; (*c*) M. Tantiwiwat, A. Tamayo, N. Luu, X.-D. Dang and T.-Q. Nguyen, *J. Phys. Chem. C*, 2008, **112**, 17402; (*d*) H. Bronstein, Z. Chen, R. S. Ashraf, W. Zhang, J. Du, J. R. Durrant, P. S. Tuladhar, K. Song, S. E. Watkins, Y. Geerts, M. M. Wienk, R. A. J. Janssen, T. Anthopoulos, H. Sirringhaus, M. Heeney and I. McCulloch, *J. Am. Chem. Soc.*, 2011, **133**, 3272; (*e*) J. C. Bijleveld, A. P. Zoombelt, S. G. J. Mathijssen, M. M. Wienk, M. Turbiez, D. M. Leeuw and R. A. J. Janssen, *J. Am. Chem. Soc.*, 2009, **131**, 16616.
7 (*a*) S. Y. Qu, W. J. Wu, J. L. Hua, C. Kong, Y. T. Long and H. Tian, *J. Phys. Chem. C*, 2010, **114**, 1343; (*b*) C. Kanimozhi, P. Balraju, G. D. Sharma and S. Patil, *J. Phys. Chem. C*, 2010, **114**, 3287; (*c*) J. Warnan, L. Favereau, Y. Pellegrin, E. Blart, D. Jacquemin and F. Odobel, *J. Photochem. Photobiol., A*, 2011, **226**, 9; (*d*) S. Y. Qu, C. J. Qin, A. Islam, Y. Z. Wu, W. H. Zhu, J. L. Hua, H. Tian and L. Y. Han, *Chem. Commun.*, 2012, **48**, 6972; (*e*) S. Y. Qu, B. Wang, F. L. Guo, J. Li, W. J. Wu, C. Kong, Y. T. Long and J. L. Hua, *Dyes Pigm.*, 2012, **92**, 1384; (*f*) J.-H. Yum, T. W. Holcombe, Y. Kim, J. Yoon, K. Rakstys, M. K. Nazeeruddin and M. Grätzel, *Chem. Commun.*, 2012, **48**, 10727; (*g*) T. W. Holcombe, J.-H. Yum, J. Yoon, P. Gao, M. Marszalek, D. Di Censo, K. Rakstys, M. K. Nazeeruddin and M. Grätzel, *Chem. Commun.*, 2012, **48**, 10724.
8 D. Cao, Q. Liu, W. Zeng, S. Han, J. Peng and S. Liu, *J. Polym. Sci., Part A: Polym. Chem.*, 2006, **44**, 2395.
9 P. Wang, S. M. Zakeeruddin, P. Comte, R. Charvet, R. Humphry-Baker and M. Grätzel, *J. Phys. Chem. B*, 2003, **107**, 1436.
10 S. Ito, T. N. Murakami, P. Comte, P. Liska, C. Grätzel, M. K. Nazeeruddin and M. Grätzel, *Thin Solid Films*, 2008, **516**, 4613.
11 E.-Q. Guo, P.-H. Ren, Y.-L. Zhang, H.-C. Zhang and W.-J. Yang, *Chem. Commun.*, 2009, 5859.
12 M. Grätzel, *Nature*, 2001, **414**, 338.
13 A. Hagfeldt, G. Boschloo, L. Sun, L. Kloo and H. Pettersson, *Chem. Rev.*, 2010, **110**, 6595.